Inorganica Chimica Acta 391 (2012) 75–82

Contents lists available at SciVerse ScienceDirect

Inorganica Chimica Acta

journal homepage: www.elsevier.com/locate/ica

Highly selective and “green” alcohol oxidations in water using aqueous 10% H_2O_2 and iron-benzenetricarboxylate metal–organic gel

Hassan Hosseini-Monfared [a,*,1], Christian Näther [b], Heiner Winkler [c], Christoph Janiak [a,*]

[a] *Institut für Anorganische Chemie und Strukturchemie, Universität Düsseldorf, Universitätsstr. 1, D-40225 Düsseldorf, Germany*
[b] *Institut für Anorganische Chemie, Universität Kiel, Olshausenstr. 40, 24098 Kiel, Germany*
[c] *Universität zu Lübeck, Institut für Physik, Ratzeburger Allee 160, D-23538 Lübeck, Germany*

ARTICLE INFO

Article history:
Received 28 February 2012
Received in revised form 5 May 2012
Accepted 10 May 2012
Available online 22 May 2012

Keywords:
Metal–organic gel
Iron
Hydrogen peroxide
Oxidation catalysis
Alcohol

ABSTRACT

A metal–organic-gel catalyst based on $Fe(NO_3)_3$ and benzene-1,3,5-tricarboxylic acid (H_3BTC) was synthesised and characterized by IR, elemental analysis, thermogravimetry/mass spectrometry (TG/MS), Mössbauer spectroscopy and environmental scanning/transmission electron microscopy (ESEM/TEM). The Fe-BTC metal–organic gel activity was evaluated for the oxidation of primary and secondary alcohols with dilute aqueous 10% H_2O_2 in water at 90 °C to the corresponding aldehydes or ketones with high chemoselectivity and with absence of overoxidation to carboxylic acids. The Fe-BTC gel catalyst allows to use only water as solvent and does not require any organic solvents. The inexpensive and non-toxic iron catalyst works with environmentally friendly hydrogen peroxide at safe, low 10% aqueous H_2O_2 concentration without the use of phase transfer conditions. A progressive addition of hydrogen peroxide significantly improved the conversion of benzyl alcohol.

1. Introduction

Selective oxidation of alcohols to carbonyl compounds is a fundamental transformation in organic synthesis because the target molecules can be obtained directly in one-pot sequences and they are important precursors for various chemicals [1–3]. Many catalytic methods have been developed for oxidation of alcohols based on different transition metals such as Pd [4–6], Cu [7], Ru [8], Co [9] and Au [10,11]. Photocatalytic oxidation of benzyl alcohol has been reported by using O_2/TiO_2 and modified O_2/TiO_2 [12]. However, most of these reported systems suffer from high reagent load, stringent reaction conditions and high cost or toxicity of the metal. Now there is a scientific challenge for chemists both in industry and academia [13] to develop more efficient, cheaper, chemoselective, and greener oxidation processes [14].

A “green” oxidation process, using hydrogen peroxide or, ideally, molecular dioxygen as the oxidant, is the most attractive oxidation technology for selective organic syntheses [15,16]. Hydrogen peroxide is a favorable and clean oxidant for various oxidation reactions [17]. It overcomes the disadvantage of the traditional toxic inorganic oxidants [18], like MnO_4^- [19]. Besides, it provides a high content of active oxygen species with water as the sole byproduct, and it is much cheaper and safer than organic peroxides or peracids. The utilization of peroxides as surrogates of dioxygen has been extensively investigated for the oxidation of various organic substrates, including amines, sulfides, alkanes, alkenes or alcohols [20,21].

Iron-containing enzymes found in nature inspired the use of iron in catalyst design [22]. The cytochrome P450 enzyme family contains an iron porphyrin heme cofactor, which oxidizes a range of organic substances in living organisms [23,24]. Non-heme enzymes such as methane monooxygenase catalyze similar oxidation reactions [25]. Iron has a number of advantages over other transition metals typically employed in catalysis; it is relatively non-toxic, abundant, cheap and environmentally friendly [14]. Consequently during the last decades, iron has become broadly used for a multitude of redox processes. Apart from reductions [26], various iron systems have been reported for epoxidation [14,27], sulfoxidation [28], hydroxylation [29], as well as oxidation of arenes to phenols and quinines [30,31]. Although iron performs well in nature, the difficulty to prevent non-selective radical reactions makes its usage for organic synthesis more difficult [21,32]. Compared with enzyme catalysts, porous materials such as zeolites [33,34], modified open-structure microporous aluminophosphates (AlPOs) [35], metal–organic frameworks (MOFs) [36] and gels [37] are interesting for catalytic oxidation, because these frameworks

---

* Corresponding authors. Address: Institut für Anorganische Chemie und Strukturchemie, Universität Düsseldorf, Universitätsstr. 1, D-40225 Düsseldorf, Germany.

E-mail addresses: monfared@znu.ac.ir (H. Hosseini-Monfared), janiak@uni-duesseldorf.de (C. Janiak).

[1] Permanent address: Department of Chemistry, University of Zanjan 45195 313, Zanjan, Iran

0020-1693/$ - see front matter © 2012 Elsevier B.V. All rights reserved.
http://dx.doi.org/10.1016/j.ica.2012.05.007

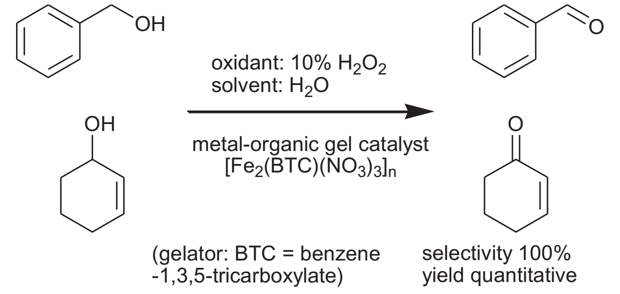

Scheme 1. The "green" catalysis route from combination of safe 10% H_2O_2 oxidant, water as solvent and a simple Fe–gel catalyst for the selective and quantitative alcohol oxidation as described in this work.

could prevent entrapped metal complexes from dimerizing and degrading [38] and also allow for control of the reactivity and selectivity of the system through the microenvironment created by the frameworks [39].

In order to prevent the formation of unwanted waste and toxic reagents, the use of inexpensive and less toxic iron complexes together with hydrogen peroxide represents an ideal combination for such oxidations. In general, chemoselectivity is the key issue for these reactions due to potential non-selective Fenton- or Gif-type chemistry (H_2O_2–Fe^{n+}) [40–42].

Several systems have been described employing different kinds of iron catalyst with H_2O_2 for the selective oxidation of alcohols and olefins; namely Fe(III)-porphyrin [43], dinuclear Fe complexes [44], Fe(III) salt [45], in situ generated thymine-1-acetate iron(III) complex [46], supported Fe_2O_3 nanoparticles (300 W microwave-assisted) [47], iron(II)-iminopyridine complexes [48], H_2O_2/nano-γ-Fe_2O_3 [49], H_2O_2/$Fe(NO_3)_3$ with pH-buffer to increase the selectivity [50] and nanoparticulare Fe_2O_3 [51] However, they need stringent reaction conditions and high cost of the ligand and multistep synthesis, or have the disadvantages like low oxidation rate and low turn-over number. Therefore, the development of practical, inexpensive, simple and green chemical processes for oxidation is still needed.

Here we report the use of a simple and inexpensive iron(III)-benzenetricarboxylate (Fe-BTC) metal–organic gel, originally synthesized by Wie and James [52], as a catalytic system for the oxidation of alcohols with 10% H_2O_2 in water (Scheme 1). The BTC ligand (cf. Fig. 1) features prominently in MOF compounds [36].

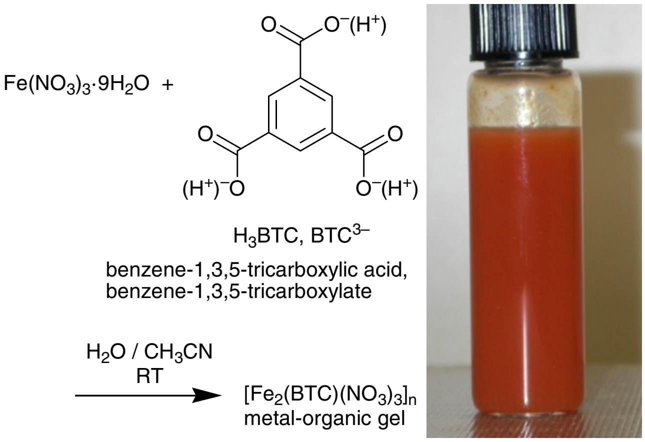

Fig. 1. Synthetic route to and appearance of Fe-BTC metal–organic gel, as synthesised before separating its solvent by centrifugation. The gel remains in this state without any precipitation even after 24 h.

2. Experimental

2.1. General

2.1.1. Materials

Reagents and solvents were purchased from the given suppliers and used without further purification: $Fe(NO_3)_3{\cdot}9H_2O$ (99.8%), benzene-1,3,5-tricarboxylic acid (95%) (H_3BTC), benzaldehyde (98%), benzyl alcohol (99%), cyclohexanol (99%), cyclohexanone (99%) and ethanol (p.a.) from Merck; acetonitrile (99.5%) 2-phenylethyl alcohol (99%), 3-buten-1-ol (96%) from Sigma–Aldrich; phenylacetaldehyde (98%), DL-*sec*-phenylethyl alcohol (1-phenylethanol) (98%), from Acros and 2-cyclohexen-1-ol (95%), acetophenone (99.5%) and 2-cyclohexen-1-one (98%) from Riedel-de-Haën. Aqueous H_2O_2 (35%) was from Solvay from which a 10% base solution was prepared. Aqueous 10% w/w hydrogen peroxide was verified to be 3.07 mol/l upon titration with potassium permanganate solution. For the titrations the H_2O_2 sample was diluted, if necessary, its pH adjusted to about 0 by addition of a few ml of conc. H_2SO_4 (c = 18 mol/l). A 0.05 mol/l $KMnO_4$ solution was used as the titrator [53]. Synthetic and spectroscopic procedures were conducted under aerobic conditions.

2.1.2. Instrumentation

For the addition of hydrogen peroxide in the catalytic oxidation experiments an automatic buret Metrohm 716 DMS Titrino was used. IR spectra (KBr pellet) were measured on a Bruker Optik IFS 25. CHN-Elemental analyses were obtained on a VarioEL from Elementaranalysensysteme GmbH. Iron analyses were carried out by atomic absorption spectrometry (AAS, Analytik Jena-Vario 6) (see Supporting information), titration with titriplex(III) (EDTA) (see Supporting information) or gravimetric analyses (see Supporting information) [54].

Environmental scanning electron microscope (ESEM) samples were analyzed with an ESEM2020. The Fe-BTC gel emulsion/dispersion was placed on a polished brass metal substrate surface to follow the drying process (see Supporting information). Alternatively, the dried Fe-BTC sample were put on a C-pad as substrate, sputtered with 24 nm gold coating or on a copper grid. The ESEM measurements were typically performed at 5–7 Torr, 5 °C and at 23 kV voltage using an ETD detector.

Transition electron microscopy (TEM) photographs were taken at room temperature from a carbon coated copper grid on a Zeiss LEO 912 transmission electron microscope operating at an accelerating voltage of 120 kV. The Fe-BTC gel emulsion sample was loaded on holey, carbon coated copper grids and dried at room temperature.

Electron spray ionization mass spectroscopy (ESI–MS) was carried out using a Finnigan MAT LCQ Advantage. MeOH was used as the solvent. Mass spectra were measured in positive and negative mode in the range of m/z = 200–2000.

^{57}Fe Mössbauer spectra were recorded with a conventional spectrometer in constant-acceleration mode with a ^{57}Co[Rh] source. The velocity calibration was performed with an α-Fe foil at room temperature, for which the magnetic hyperfine splitting is known with high accuracy. The measured isomer shifts are referred to this α-Fe standard. The experimental spectra were fitted by a sum of Lorentzian lines by means of a least-squares procedure.

DTA–TG/MS instrumentation: STA-409CD with skimmer coupling from Netzsch, quadrupole mass spectrometer QMA 400 from Balzers. The MS measurements were performed in analog and trend scan mode. All measurements were corrected for buoyancy and current effects and were performed using heating rates of 4 °C min^{-1}. in Al_2O_3 crucibles in a dynamic helium atmosphere (purity 4.6; flow-rate: 75 ml min^{-1}.). The thermobalance was calibrated using standard reference materials.

2.2. Preparation of Fe-BTC gel

The preparation was carried out following a brief protocol in Ref. [52] with slight solvent modification. Solutions of Fe$(NO_3)_3{\cdot}9H_2O$ (12.10 g, 30.0 mmol) in 75 ml of acetonitrile–water 1:1 (v/v) and H_3BTC (2.10 g, 10.0 mmol) in 100 ml acetonitrile–water 1:1 (v/v) were rapidly mixed together and instantly a brown gel was formed. After 5 min of stirring the gel was collected by centrifugation (10 min, 2000 rpm) and decantation of the supernatant solvent. Gelation was confirmed by the inverted test-tube method [52]. Gel formation was reproducibly repeated 10 times. Part of the gel was dried at 50 °C under vacuum for 8.5 h. After grinding this dried gel to a fine powder in a mortar, drying was continued under vacuum at 100 °C for 5.5 h. *Anal.* calc. for $[Fe_2(C_9H_3O_6)(NO_3)_3(H_2O)_3]$ (558.88) calcd. C, 19.34: H, 1.62: N, 7.52: Fe, 19.99. Found: C, 18.87: H, 1.56: N, 7.38: Fe, 20.1%. IR (KBr, cm^{-1}): 3421 (m), 2923 (s), 2854 (m), 2362 (w), 1720 (m), 1634 (m), 1455 (w), 1384 (vs), 1307 (w), 1239 (s), 1153 (m), 983 (w), 754 (w), 711 (w), 621 (w), 419 (m).

2.3. Alcohol oxidation, general procedure

Special care was taken to conduct a series of experiments under identical conditions. The oxidant H_2O_2 (5, 10 or 35% w/w, corresponding to 1.83, 3.07 or 11.0 mol/l, respectively) was added through a syringe pump with a chosen constant rate (between 0.06 and 0.20 ml min^{-1}) to an aqueous mixture (5 ml) containing the dried Fe-BTC gel (10 mg, 36 μmol Fe, 18 μmol $[Fe_2(C_9H_3O_6)(NO_3)_3(H_2O)_3]$ catalyst) and benzyl alcohol (1.00 g, 9.26 mmol). During H_2O_2 addition the mixture was stirred in a 50 ml three neck round bottom flask at a rate of 1300 rpm while the temperature (RT, 60 or 90 °C) was kept constant. Reaction conversion was monitored by GC/MS analysis of 0.20 ml aliquots withdrawn periodically from the reaction mixture. Yields were based on GC/MS analysis only. The products were not isolated. For the GC/MS analysis the sample was homogenized by adding 0.2 ml ethanol. All catalytic reactions were run at least three times and analyzed by GC/MS and the average conversion yields are presented. Conversion was based on the consumption of the starting alcohol together with the amount of the aldehyde or ketone product.

For the GC/MS analysis an HP 5890 Series II GC fitted with an Ultra2 column (stationary phase Ph-Me-silicone, 45 m, outer diameter 0.2 mm, inner diameter 0.11 mm, carrier gas He) and connected to a quadrupole mass spectrometer HP 5989A (EI ionization) was employed. The area ratios of the alcohol starting material and the aldehyde or ketone product were calibrated by using 2:1, 1:1, 1:0.5 (mol/mol) mixtures of the genuine substances. For example, at a 1:1 M ratio the area ratio was not 1, so the calibration curve was needed to convert the experimental area ratio to the starting material and product substance percentage. Calibration curve was obtained by drawing product/alcohol area ratio against product percent in solution. Only with the calibration curve a direct and linear correlation was obtained between area ratio and the product or reactant percentage.

3. Results and discussion

3.1. Synthesis and characterization

Fe(III)-containing gels are easily prepared by mixing $Fe(NO_3)_3$ and H_3BTC solutions in 1/1 (v:v) mixture of CH_3CN/H_2O instantly within 2 min [52]. This gel is stable for months and its physical state remains the same without any precipitate formation if excess solvent is not removed by centrifugation (Fig. 1). Formation of the gel is caused by entrapping solvent molecules into the spaces of the three-dimensional covalent and/or hydrogen-bonded network created by the benzenetricarboxylate or benzenetricarboxylic acid metallogelator [55]. The gel does not dissolve in water at room temperature.

Fig. 2. Solidified gel after drying at 100 °C for 5.5 h as it was used in the catalytic oxidation reactions.

Various methods for preparing single crystals of Fe^{3+} and H_3BTC were examined but failed (see Supporting information). To allow for a defined mass of the metal–organic gel to be used in catalysis, the gel was dried at 50 °C under vacuum for 8.5 h. After grinding this dried gel to a fine powder in a mortar, drying was continued under vacuum at 100 °C for 5.5 h to give an orange-brown glassy solid (Fig. 2). The dried gel was ground well for a high surface area but not too small for a convenient filtration after catalytic use.

The drying process could also be followed by environmental scanning electron microscopy (ESEM, see Fig. S1 in Supporting information). A transmission electron micrograph (TEM) of a room temperature dried Fe-BTC gel sample from the emulsion shows isolated dispersion particles with very good resolution. The main particle size is about 150 nm but smaller particles of less than 50 nm are also present (Fig. 3).

When dried under vacuum at 100 °C for 5.5 h the particles aggregate. Yet, ESEM investigations of the dried samples reveal the build-up of these aggregates from smaller particles (Fig. 4).

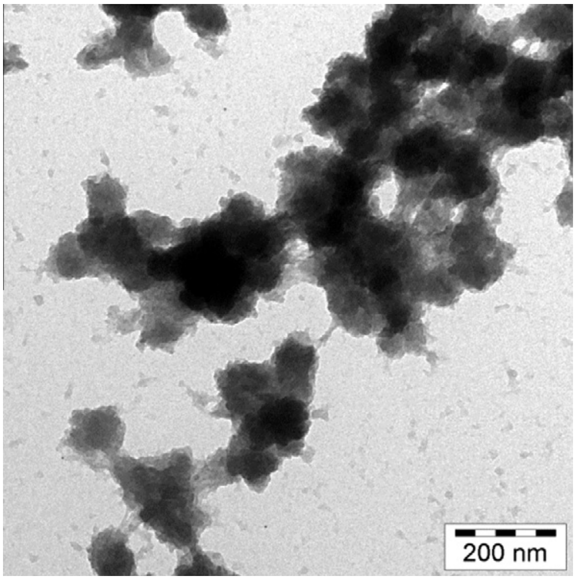

Fig. 3. TEM image of a Fe-BTC sample dried at room temperature on carbon-coated copper grid; see Fig. S2 in Supporting information for additional TEM pictures.

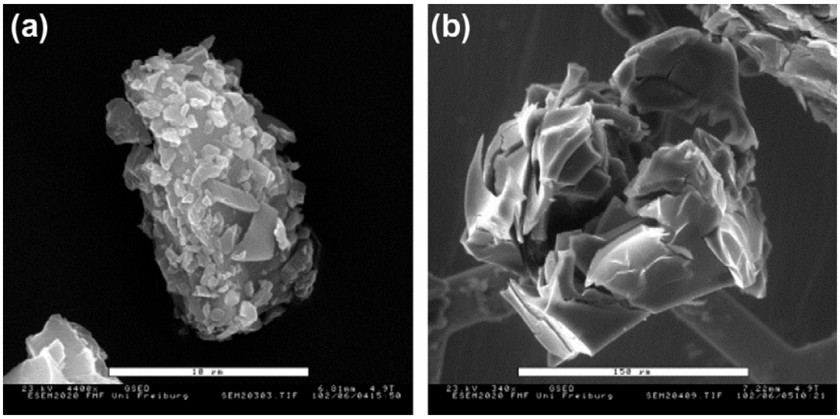

Fig. 4. ESEM of a Fe-BTC sample after drying at 100 °C for 5.5 h. (a) Particles on C-pad as substrate and sputtered with 24 nm gold coating and (b) particles on a copper grid. Additional ESEM pictures are given in Figs. S3 and S4 in Supporting information.

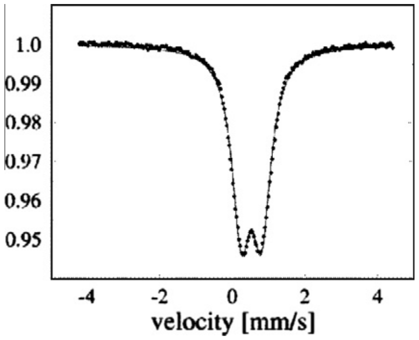

Fig. 5. Mössbauer spectrum of dried Fe-BTC gel at T = 77 K. A sum of Lorentzians (solid line, parameters in text) is used to fit the experimental data (dots).

ESI–MS spectra of the solution phase of the dried gel dispersed in methanol gave in positive ion mode major signals at m/z = 327, 591 and 679 corresponding to $[Fe(H_2BTC)NO_3]^+$, $[Fe_2(BTC)(HBTC)(CH_3OH)_2]^+$ and $[[Fe_3(BTC)_2(NO_3)(OH)(H_2O)]^+$, respectively, with $[Fe(H_2BTC)NO_3]^+$ as the most intense signal (Fig. S5 in Supporting information).

A Mössbauer spectrum for the dried Fe-BTC gel is shown in Fig. 5. At 77 K, the Mössbauer parameters were δ = 0.53 mm/s and Δ_{EQ} = 0.56 mm/s indicating an octahedral high-spin Fe(III) (S = 5/2) center, with the iron bound to O-atom donors [56]. For high-spin Fe(III) the observed isomer shift ($\delta^{\alpha\text{-Fe}} < 0.6$ mm s^{-1}) and small quadrupole splitting are typical [57,58]. Note that even though there is a symmetric charge distribution of high-spin d^5-Fe(III), there is a contribution for a small quadrupole splitting from the ligand field which is of lower than O_h symmetry (D_{4h} for a *trans*-FeO_4O_2' coordination and D_{2h} for a $FeO_2O_2'O_2''$ coordination if the differences between benzenetricarboxylato, nitrato and aqua ligands are taken into account) [59]. The full width at half-height (Γ = 0.61 mm/s) is only slightly broader than in defined molecular Fe(III) complexes (theoretical width ~0.35 mm/s) and still within the range of widths observed for the high-spin component of Fe(III) spincrossover complexes [57]. This indicates very similar pseudo-octahedral Fe(III)–oxygen environments or a very uniform Fe-sample. We rule out the presence of different Fe(III) species, e.g. in the form of $Fe(NO_3)_3$ aq starting material (see also below in Section 3.2).

Investigations using simultaneous differential thermoanalysis and thermogravimetry coupled to mass spectroscopy (DTA–TG/MS) of the dried Fe-BTC gel (Fig. 6) do not yield a well-resolved TG curve which precludes a good quantitative analysis. Still, the dried gel does not show any loss of acetonitrile (CH_3CN) which was used as solvent during the synthesis (Fig. 1). A first TG step derives from the water (m/z = 18) loss of the sample. Further heating leads to formation of NO (m/z = 30) and NO_2 (m/z = 46, not shown) due to nitrate decomposition. At 350 °C a plateau is reached with $\Delta m \approx -38\%$ before further mass loss resumes with loss of CO_2 (m/z = 44) and presumably benzene (m/z = 78) of $\Delta m \approx -33\%$ to a total mass loss of −71.5% at 600 °C. In agreement with elemental analysis (see Section 2) an assumed sum formula of $[Fe_2(C_9H_3O_6)(NO_3)_3(H_2O)_3]$ for the dried gel is largely in accordance with a mass loss of H_2O (9.6%) + NO_3(33.3%) − xO (remaining as Fe_2O_3) to yield the first step of $\Delta m \approx -38\%$ until 350 °C. The loss of $C_9H_3O_6$ (37%) − yO (remaining as Fe_2O_3) then accounts for the second step between 375 and 600 °C. The residue amount is in accord to remaining Fe_2O_3 (Δm_{exp}: 28.5%, Δm_{theor}: 28.6%). The residue is amorphous proven by X-ray powder diffraction.

3.2. Catalytic activity

We first examined the catalytic activities of the dried Fe-BTC gel toward hydrogen peroxide oxidation of benzyl alcohol in H_2O as a

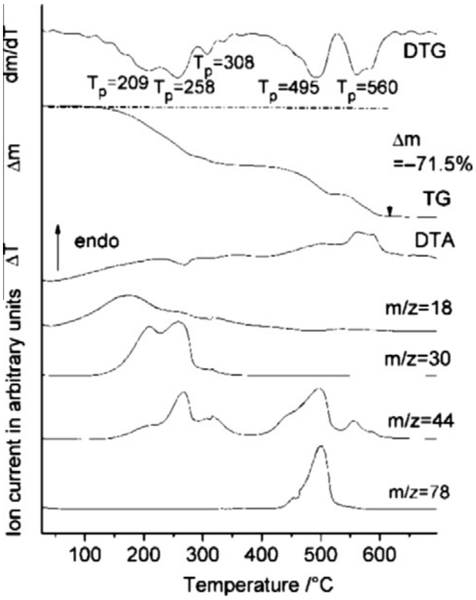

Fig. 6. DTG, TG, DTA and MS trend scan curves for m/z = 18 (H_2O), 30 (NO), 44 (CO_2) and 78 (presumably C_6H_6) (from top to bottom) for dried Fe-BTC gel; values refer to the peak temperature (T_p) in °C (DTG) and to the mass loss in % (TG) (Al_2O_3 crucible, He atmosphere; 75 ml min^{-1}).

Table 1
Effect of hydrogen peroxide concentration and addition rate on the oxidation of benzyl alcohol by Fe-BTC gel.[a]

Entry	Temp. (°C)	Total H_2O_2-Vol./ml (conc.)	H_2O_2 addition rate (ml min^{-1})	Time (min)	TON [b]	Conversion (%)
1	25	3.4 (35%)	at once	420	10	2
2	25	20 (35%)	0.12	420	10	2
3	60	3 (35%)	at once	300	118	23
4a	90	10.8 (10%) [c]	0.06	180	447	87
4b	90	12.6 (10%) [c]	0.06	210	463	90
5a	90	20 (10%) [d]	0.12	180	504	98
5b	90	20 (10%) [d]	0.12	210	514	quant.
6	90	18 (5%) [e]	0.10	180	252	49
7	90	20 (5%) [e]	0.20	180	421	82
8	90, no cat.	3.4 (35%)	at once	240	<10	<2

[a] Conditions: dried Fe-BTC gel 0.010 g (2 mg Fe, 36 μmol Fe, 18 μmol $[Fe_2(C_9H_3O_6)(NO_3)_3(H_2O)_3]$ catalyst); benzyl alcohol 9.26 mmol; molar ratio benzyl alcohol/Fe = 9.26/0.036 = 257; aqueous 35% H_2O_2 c = 11 mmol/ml; aqueous 10% H_2O_2 c = 3.07 mmol/ml; aqueous 5% H_2O_2 c = 1.83 mmol/ml; H_2O 5 ml.

[b] TON = turnover number [mol product/mol catalyst], the turnover frequency TOF [mol product/(mol catalyst × time)] is obtained by dividing TON through time.

[c] Molar ratio H_2O_2/benzyl alcohol = 3.3.

[d] Molar ratio H_2O_2/benzyl alcohol = 6.6.

[e] Molar ratio H_2O_2/benzyl alcohol = 3.9.

test reaction. Benzyl alcohol was taken as a model substrate for oxidation activity studies of the Fe-BTC gel/H_2O_2 system because of its solubility in water. In addition, benzaldehyde is an interesting target molecule, since it is easily over-oxidized to benzoic acid, therefore, the formation of benzoic acid is a direct measure of the selectivity of the protocol. At room temperature oxidation of benzyl alcohol with aqueous 35% H_2O_2 was not catalyzed (conversion 2%) by the gel even after 420 min (7 h, entry 1, Table 1). In general, the Fe-BTC gel does not appear to activate H_2O_2 at room temperature but only at elevated temperature. Increasing the H_2O_2 amount (entry 2) or the gel concentration did not improve the conversion at room temperature. Therefore, we can also rule out the presence of $Fe(NO_3)_3$ aq starting material as soluble Fe(III) species leading to Fe^{3+}(aq) ions decompose H_2O_2 instantly [60]. The dried Fe-BTC gel was, however, found to effectively catalyze the oxidation of benzyl alcohol to benzaldehyde by hydrogen peroxide above room temperature at 60 or 90 °C.

By adding 3 ml of aqueous 35% H_2O_2 at once at 60 °C, the benzyl alcohol oxidation was 23% after 300 min (entry 3, Table 1). $KMnO_4$ tests proved the absence of H_2O_2 in the reaction mixture after this time. In addition, when 3 ml of aqueous 35% H_2O_2 was added in small portions at 60 °C the substrate conversion increased (not given in Table 1). Both of these results indicate a catalase-like dismutation of H_2O_2 by Fe-BTC gel. Consequently, two main reactions, namely the substrate oxidation and the H_2O_2 dismutation, are competing. Previously, iron(III) complexes with porphyrin/phenolate [61] and tetraaza[14]annulenes [62] ligands have been shown to be catalase models. Because of the second reaction order in hydrogen peroxide in catalase-type dismutation (two molecules of H_2O_2 are required to produce one molecule of O_2) a decrease of the local H_2O_2 concentration should strongly disfavor the dismutation reaction with respect to the catalytic oxidation. Therefore we added the oxidant progressively with the help of a Metrohm microburette a 90 °C. Quantification of H_2O_2 concentration with $KMnO_4$ confirmed that aqueous H_2O_2 is stable in the presence of the reactant and the absence of dried Fe-BTC gel at room temperature, 60 or 90 °C. Benzaldehyde and H_2O_2 in absence of the Fe-BTC catalyst showed only 1% alcohol-to-aldehyde conversion in 240 min (entry 8, Table 1).

Various addition rates (0.06–0.20 ml min^{-1}) and concentrations of H_2O_2 (5%, 10% and 35%) were used. Conversion depended on both the H_2O_2 concentration and its addition rate. An addition rate for 10% H_2O_2 of 0.06 ml min^{-1} already gave a good conversion to 87% in 180 min (entry 4, Fig. 7a). Increasing the addition rate for 10% H_2O_2 to 0.12 ml min^{-1} gave near quantitative (98%) conversion in 180 min and no more benzaldehyde could be seen by GC/MS after 210 min (quantitative conversion) (entry 5, Fig. 7b).

Similarly for 5% H_2O_2 at an addition rate of 0.10 ml min^{-1} conversion proceeded slowly up to 49% after 180 min (entry 6, Fig. 7c) but continuous without any further addition to 85% within 1020 min (17 h, not shown). By increasing the addition rate for 5% H_2O_2 to 0.20 ml min^{-1} the oxidation rate increased to a conversion of 82% after 180 min (entry 7). However, the conversion was incomplete even after 240 min (Fig. 7d). Thus, a concentration of 5% H_2O_2 was too low for effective oxidation.

During the beginning of the oxidation reaction, the gel remains solid-like and heterogeneous. However, after 15–20 min because of vigorous stirring at a temperature of 90 °C the gel disperses and a yellow colloidal solution resulted, with or without alcohol and H_2O_2. This indicates that the catalytic action is not truly heterogeneous but that the gel serves as a reservoir for the slow release of active "homogeneous" iron-species into solution at higher temperatures than room temperature (see above). Vigorous stirring was necessary because the organic alcohol reactant and aldehyde product are not fully miscible with water. At room temperature the organic benzyl alcohol phase separates at the bottom of the flask (density = 1.05 g/cm^3). Hence, sampling for the GC measurements was carried out when the oxidation mixture was stirred vigorously. After cooling the reaction mixture to room temperature, the dispersed gel precipitated again as an orange-brown solid. By freezing the mixture, the gel precipitation increased. The Fe-BTC gel was separated by decanting the supernatant solution.

The possibility of recycling the Fe-BTC gel and re-using it as a catalyst was checked with benzyl alcohol as the reactant. The oxidation of benzyl alcohol with the recycled gel decreased to 20% conversion (20 ml 10% H_2O_2, 0.12 ml min^{-1}, 180 min). Recycling the gel three times decreased the benzyl alcohol conversion to 10% even when increasing the reaction time to 360 min (6 h).

Over-oxidation was not seen in Fe-BTC gel catalyzed oxidation of benzyl alcohol as the only product was benzaldehyde with >99% selectivity (entry 1, Table 2). In some reported systems of Fe(III)-Schiff base/H_2O_2 a large excess of substrate to H_2O_2 (molar substrate:H_2O_2 ratio 1000:20) has been used to minimize over-oxidation of oxidation products [63]. A slight drawback of the Fe-BTC gel system is the need for a 3- to 6.6-fold excess of hydrogen peroxide relative to substrate. The excess consumption of H_2O_2 is attributed to the competitive parallel reaction of hydrogen peroxide decomposition promoted by the catalyst (catalase-like activity). This situation has been also reported for Mn(III) and Mo(IV)-salen complexes immobilized on mesoporous silica gel [64] and oxidant requirement of the H_2O_2/cyclooctene ratio of 10 order in epoxidation reactions [65,66].

After demonstrating the selective oxidation of benzyl alcohol, we evaluated the Fe-BTC gel in the oxidation of other alcohols by

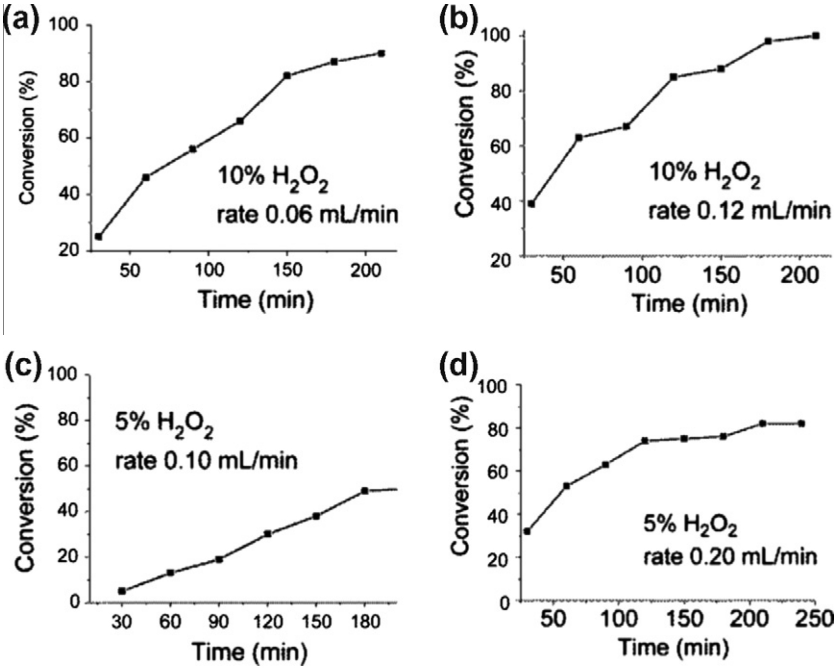

Fig. 7. Oxidation of benzyl alcohol by Fe-BTC and progressive addition of different H_2O_2 concentration at different rates; see Table 1 for further details.

Table 2
Fe-BTC gel catalyzed oxidation of various alcohols.[a]

Entry	Substrate	Product(s)	Selectivity (%)	Time (min)	TON [b]	Conversion (%)
1	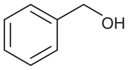	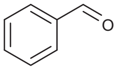	>99	180	504	98
2	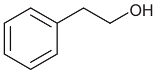	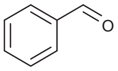	48	180	118	23
		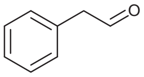	52			
3	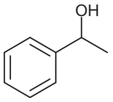	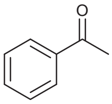	>99	30 180	288 514	56 100
4	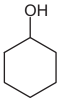	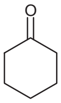	>99	60 120 150	200 339 375	39 66 73
5	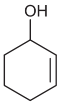	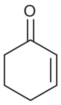	>99	60 120	175 267	34 52

[a] Conditions: dried Fe-BTC gel 0.010 g (2 mg Fe, 36 μmol Fe, 18 μmol $[Fe_2(C_9H_3O_6)(NO_3)_3(H_2O)_3]$ catalyst), alcohol 9.26 mmol, molar ratio alcohol/Fe = 9.26/0.036 = 257; total H_2O_2-volume 20 ml of 10% H_2O_2 (c = 3.07 mmol/ml) at an addition rate of 0.12 ml min^{-1}; H_2O 5 ml; molar ratio H_2O_2/alcohol = 6.6.

[b] TON = turnover number [mol product/mol catalyst], the turnover frequency TOF [mol product/(mol catalyst x time)] is obtained by dividing TON through time.

using 20 ml 10% H_2O_2 at an addition rate of 0.12 ml min^{-1} as standard procedure (Table 2). The oxidation of 2-phenyl ethanol resulted in 23% conversion after 3 h with almost equal ratio of benzaldehyde and 2-phenylacetaldehyde (entry 2). From 1-phenylethanol and cyclohexanol the corresponding ketones were obtained with an excellent selectivity of more than 99% for acetophenone or cyclohexanone, respectively (entry 3 and 4, Table 3). Conversion of the benzylic alcohol 1-phenylethanol was quantitative within 180 min. Also the oxidation of the allylic alcohol 3-cyclohexenol (entry 5, Table 3) proceeded with excellent selectivity of >99% to cyclohexenone but at moderate conversion of 52%. In all cases no other side-products than those stated could be identified.

The aforementioned Fe-BTC gel catalytic accomplishments have to be seen in comparison to other Fe-catalysts from the literature. Various Fe(II)/Fe(III)-catalysts have been used for the oxidation of cyclohexanol, 1-phenyl ethanol, benzyl alcohol and cyclohex-2-enol with H_2O_2 and t-BuOOH (Table 3). None of the catalysts shows a high activity and selectivity like the Fe-BTC gel catalyst. An exception is the catalyst $[FeCl_2(Py_2S_2)]$ (1,6-bis(2′-pyridyl)-2,5-dithiahexane=Py_2S_2) which shows high activity in the oxidation of 1-phenyl ethanol to acetophenone

Table 3
Oxidation characteristics of various alcohols by different Fe catalysts.

Entry	Substrate to product	Conversion (%)	Selectivity[a] (%)	Time (min)	Oxidant/catalyst	TOF [g] (h^{-1})	References
1	cyclohexanol to cyclohexanone	73	100	150	H_2O_2/Fe(III)-BTC gel	150	this work
2		36	100	240	t-BuOOH/Fe(II)-Py_2S_2/MW [b]	45	[67]
3		56	99	30	H_2O_2/Fe(II)-L3-Na_2CO_3 [c]	22	[68]
4		70	100	90	H_2O_2/Fe(III)-Schiff base[d]	12	[69]
5	1-phenyl ethanol to acetophenone	56	100	30	H_2O_2/Fe(III)-BTC gel	576	this work
6		80	100	15	t-BuOOH/Fe(II)-Py_2S_2/MW [b]	1602	[67]
7		65	99	60	H_2O_2/Fe(II)-L3-Na_2CO_3 [c]	13	[69]
8	benzyl alcohol to benzaldehyde	100	100	210	H_2O_2/Fe(III)-BTC gel	171	this work
9		84	90	30	H_2O_2/Fe(II)-L3-Na_2CO_3 [c]	34	[69]
10		80	100	90	H_2O_2/Fe(III)-Schiff base [d]	13	[70]
11		72	66	12 h	H_2O_2/nano-γ-Fe_2O_3 [e]	1	[49]
12		89	89	12 h	H_2O_2/$Fe(NO_3)_3$/KH_2PO_4 [f]	4	[50]
13	cyclohex-2-enol to cyclo-2-enone	52	100	120	H_2O_2/Fe(III)-BTC gel	134	this work
14		99	76	30	H_2O_2/Fe(II)-L3- Na_2CO_3 [c]	40	[69]

[a] Selectivity refers to the chemoselectivity of aldehyde or ketone from alcohol.
[b] MW = microwave assisted oxidation, catalyst [$FeCl_2(Py_2S_2)$] (1,6-bis(2′-pyridyl)-2,5-dithiahexane = Py_2S_2).
[c] L3 = 6-(*N*-phenylbenzimidazoyl)-2-pyridinecarboxylic acid, Na_2CO_3, CH_2Cl_2. 0.025 mmol iron salt, substrate.
[d] Fe(III)-(triphenylphosphine)$_2$(*N*-(2-mercaptophenyl)salicylideneimine).
[e] Benzyl alcohol (10 mmol), H_2O_2 (10 mmol, 30 wt.% in water), 1 mol% of catalyst, 75 °C, 12 h. H_2O_2 was added continuously in 12 h.
[f] Benzyl alcohol (10 mmol), $Fe(NO_3)_3 \cdot 9H_2O$ (0.2 mmol), KH_2PO_4 (0–0.6 mmol), 75 °C. 15 mmol H_2O_2 (30 wt.% in water) was added continuously with a syringe pump in 12 h.
[g] Turnover frequency [mol product/(moles metal catalyst × hour)] = TON/(time in hour).

with t-BuOOH, under microwave assistence (entry 7, Table 3) [67].

4. Conclusions

A novel and easily prepared metal–organic Fe-BTC gel catalyst is described for the oxidation of benzylic and allylic alcohols and cyclohexanol which works with 10% aqueous hydrogen peroxide as oxidant under mild conditions. This catalyst is more efficient, cheaper, more chemoselective, hence, "greener" than comparative literature systems. So far, the Fe-BTC gel catalyst appears mainly to be effective towards reactive benzyl alcohols. In future work we will investigate the possibility to increase the Fe-BTC gel efficiency towards less active alcohols.

Despite their power as a synthetic tool and abundant use in academic research, oxidation reactions as a whole comprise as little as 3% of the reactions used on a preparative scale in the pharmaceutical industry [68]. Perhaps the greatest factor influencing the hesitation to employ oxidation reactions on a large scale is the safety of these processes. Using diluted H_2O_2 (less than 30%) and water as solvent improves oxidation process safety in large scale syntheses. Dilute aqueous hydrogen peroxide solution is a safe, non-toxic and low cost oxidant. It can readily be activated by Fe(III) complexes such as the easily and rapidly prepared Fe-BTC gel used here.

Acknowledgments

This work was in part supported by DFG Grant Ja466/23-1 (initiation of bilateral cooperation HHM-CJ). We thank Dr. Yi Thomann and Dr. Ralf Thomann for the ESEM and TEM pictures, Mrs. Lydia Walter (Institute of pharmacy) for the GC/MS analyses and the University of Zanjan for a partial fellowship to H. Hosseini-Monfared.

Appendix A. Supplementary material

Supplementary data associated with this article can be found, in the online version, at http://dx.doi.org/10.1016/j.ica.2012.05.007.

References

[1] G. Tojo, M. Fernandez, Oxidation of Alcohols to Aldehydes and Ketones, Springer, Berlin, 2006.
[2] J.E. Bäckvall (Ed.), Modern Oxidation Methods, Wiley-VCH, Weinheim, 2010.
[3] R.A. Sheldon, J.K. Kochi, In: Metal-Catalyzed Oxidation of Organic Compounds, Academic Press, New-York, 1981.
[4] S. Shimazu, T. Uehara, A. Asami, T. Hara, N. Ichikuni, J. Mol. Catal. A: Chem. 282 (2008) 28.
[5] U.R. Pillai, E. Sahle-Demessie, Green Chem. 6 (2004) 161.
[6] N. Jamwal, M. Gupta, S. Paul, Green Chem. 10 (2008) 999.
[7] I.E. Marko, A. Gautier, R. Dumeunier, K. Doda, F. Phillippart, S.M. Brown, C.J. Urch, Angew. Chem., Int. Ed. 43 (2004) 1588.
[8] G. Csjernyik, A.H. Ella, L. Fadini, B. Pugin, J.-E. Bäckvall, J. Org. Chem. 67 (2002) 1657.
[9] M. Zhao, J. Li, Z. Song, R. Desmond, D.M. Tschaen, E.J.J. Grabowski, P.J. Reider, Tetrahedron Lett. 39 (1998) 5323.
[10] V.R. Choudhary, A. Dhar, P. Jana, R. Jha, B.S. Uphade, Green Chem. 7 (2005) 768.
[11] C.D. Pina, E. Falletta, L. Prati, M. Rossi, Chem. Soc. Rev. 37 (2008) 2077.
[12] W. Feng, G. Wu, L. Li, N. Guan, Green Chem. 13 (2011) 3265.
[13] R.A. Sheldon, I.C.W.E. Arends, G.J. ten Brink, A. Dijksman, Acc. Chem. Res. 35 (2002) 774.
[14] G. Anilkumar, B. Bitterlich, F. Gadissa Gelalcha, M.Ki. Tse, M. Beller, Chem. Commun. (2007) 289.
[15] W. Ma, J. Li, X. Tao, J. He, Y. Xu, J.C. Yu, J. Zhao, Angew. Chem., Int. Ed. 42 (2003) 1029.
[16] A. Sorokin, B. Meunier, Chem. Eur. J. 2 (1996) 1309.
[17] Y. Ding, W. Zhao, H. Hua, B.C. Ma, Green Chem. 10 (2008) 910.
[18] S.J. Zhang, G.D. Zhao, S. Gao, Z.W. Xi, J. Xu, J. Mol. Catal. A: Chem. 289 (2008) 22.
[19] L. Kotai, B. Kazinczy, A. Keszler, H. Sandor, I. Gacs, K. Banerji, Z. Naturforsch. B 56 (2001) 823–825.
[20] H.-B. Kraatz, N. Metzler-Nolte, Concepts and Models in Bioinorganic Chemistry, Wiley-VCH, Weinheim, 2006.
[21] M. Costas, K. Chen, L. Que Jr., Coord. Chem. Rev. 200–202 (2000) 517.
[22] L. Que Jr., W.B. Tolman, Nature 455 (2008) 333.
[23] P.R. Ortiz de Montellano, Chem. Rev. 110 (2010) 932.
[24] A. Correa, O.G. Mancheno, C. Bolm, Chem. Soc. Rev. 37 (2008) 1108.
[25] P.C.A. Bruijnincx, G. van Koten, R.J.M. Klein Gebbink, Chem. Soc. Rev. 37 (2008) 2716.
[26] R. Langer, G. Leitus, Y. Ben-David, D. Milstein, Angew. Chem., Int. Ed. 50 (2011) 2120.
[27] E. Rose, E. Gallo, N. Raoul, L. Bouche, A. Pille, A. Caselli, O.J. Lequin, J. Porphyrins Phthalocyanines 14 (2010) 646.
[28] C.O. Kinen, L.I. Rossi, R.H. de Rossi, J. Org. Chem. 74 (2009) 7132.
[29] M.A. Bigi, S.A. Reed, M.C. White, Nat. Chem. 3 (2011) 216.
[30] R. Molinari, T. Poerio, Appl. Catal. A: Gen. 393 (2011) 340.
[31] H.M. Neu, V.V. Zhdankin, V.N. Nemykin, Tetrahedron Lett. 50 (2010) 6545.
[32] C. Bolm, J. Legros, J. Le Paih, L. Zani, Chem. Rev. 104 (2004) 6217.
[33] R.F. Parton, I.F.J. Vankelecom, M.J.A. Casselman, C.P. Bezoukhanova, J.B. Uytterhoeven, P.A. Jacobs, Nature 370 (1994) 541.
[34] F. Thibault-Starzyk, M.V. Puymbroeck, R.F. Parton, P.A. Jacobs, J. Mol. Catal. A: Chem. 109 (1996) 75.
[35] J.M. Thomas, R. Raja, Aust. J. Chem. 54 (2001) 551.
[36] (a) C. Janiak, J.K. Vieth, New J. Chem. 34 (2010) 2366;
(b) S.L. James, Chem. Soc. Rev. 32 (2003) 276;
(c) C. Janiak, Dalton Trans. (2003) 2781.

[37] (a) S. Xiang, L. Li, J. Zhang, X. Tan, H. Cui, J. Shi, Y. Hu, L. Chen, C.-Y. Su, S.L. James, J. Mater. Chem. 22 (2012) 1862;
(b) J. Zhang, X. Wang, L. He, L. Chen, C.-Y. Su, S.L. James, New J. Chem. 33 (2009) 1070.

[38] F. Bedioui, Coord. Chem. Rev. 144 (1995) 39.

[39] S. Evans, J.R. Lindsay Smith, J. Chem. Soc., Perkin Trans. 1 2 (2001) 174.

[40] H.J.H. Fenton, Chem. News 33 (1876) 190.

[41] D.H.R. Barton, Chem. Soc. Rev. 25 (1996) 237.

[42] D.T. Sawyer, A. Sobkowiak, T. Matsushita, Acc. Chem. Res. 29 (1996) 409.

[43] J.H. Han, S.K. Yoo, J.S. Seo, S.J. Hong, S.K. Kim, C. Kim, Dalton Trans. (2005) 402.

[44] E. Balogh-Hergovich, G. Speier, J. Mol. Catal. A: Chem. 230 (2005) 79.

[45] S.E. Martin, A. Garrone, Tetrahedron Lett. 44 (2003) 549.

[46] A. Al-Hunaiti, T. Niemi, A. Sibaouih, P. Pihko, M. Leskelä, T. Repo, Chem. Commun. 46 (2010) 9250.

[47] A.M. Balu, A. Pineda, K. Yoshida, J.M. Campelo, P.L. Gai, R. Luque, A.A. Romero, Chem. Commun. 46 (2010) 7825.

[48] P. Shejwalkar, N.P. Rath, E.B. Bauer, Dalton Trans. 40 (2011) 7617.

[49] F. Shi, M.K. Tse, M.M. Pohl, J. Radnik, A. Brückner, S. Zhang, M. Beller, J. Mol. Catal. A: Chem. 292 (2008) 28.

[50] F. Shi, M.K. Tse, Z. Li, M. Beller, Chem. Eur. J. 14 (2008) 8793.

[51] F. Shi, M.K. Tse, M.-M. Pohl, A. Brückner, S. Zhang, M. Beller, Angew. Chem., Int. Ed. 46 (2007) 8866.

[52] Q. Wie, S.L. James, Chem. Commun. 12 (2005) 1555.

[53] A.I. Vogel, Textbook of Quantitative Inorganic Analysis, fourth ed., Longman, London and New York, 1978.

[54] J. Strähle, E. Schweda, Jander-Blasius, Einführung in das Anorganisch-Chemische Praktikum, fourteenth ed., S. Hirzel, Verlag Stuttgart, 1995, p. 322ff.

[55] J. Makarević, M. Jokić, L. Frkanec, D. Katalenićć, M. Žinić, Chem. Commun. (2002) 2238.

[56] D.P.E. Dickson, F.J. Berry, Mössbauer Spectroscopy, Cambridge University Press, 1996.

[57] B. Kersting, M.J. Kolm, C. Janiak, Z. Anorg. Allg. Chem. 624 (1998) 775.

[58] B. Kersting, D. Siebert, D. Volkmer, M.J. Kolm, C. Janiak, Inorg. Chem. 38 (1999) 3871.

[59] A. Geiß, M.J. Kolm, C. Janiak, H. Vahrenkamp, Inorg. Chem. 39 (2000) 4037.

[60] H. Hosseini Monfared, Z. Amouei, J. Mol. Catal. A: Chem. 217 (2004) 161.

[61] A. Takahashi, T. Kurahashi, H. Fujii, Inorg. Chem. 48 (2009) 2614.

[62] R. Sustmann, H.-G. Korth, D. Kobus, J. Baute, K.-H. Seiffert, E. Verheggen, E. Bill, M. Kirsch, H. de Groot, Inorg. Chem. 46 (2007) 11416.

[63] G. Bilis, K.C. Christoforidis, Y. Deligiannakis, M. Louloudi, Catal. Today 157 (2010) 101.

[64] T. Luts, R. Frank, W. Suprun, S. Fritzsche, E. Hey-Hawkins, H. Papp, J. Mol. Catal. A: Chem. 273 (2007) 250.

[65] B.S. Lane, M. Vogt, V.J. DeRose, K. Burgess, J. Am. Chem. Soc. 124 (2002) (1954) 1946.

[66] S. Ueno, K. Yamaguchi, K. Yoshida, K. Ebitani, K. Kaneda, Chem. Commun. (1998) 295.

[67] R.R. Fernandes, J. Lasri, M. Fátima, C.G. da Silva, J.A.L. da Silva, J.J.R. Fraústo da Silva, A.J.L. Pombeiro, Appl. Catal. A402 (2011) 110.

[68] R.W. Dugger, J.A. Ragan, D.H. Brown Ripin, Org. Process Res. Dev. 9 (2005) 253.

[69] B. Join, K. Möller, C. Ziebart, K. Schröder, D. Gördes, K. Thurow, A. Spannenberg, K. Junge, M. Beller, Adv. Synth. Catal. 353 (2011) 3023.

[70] S. Rani, B. Ramachandra Bhat, Tetrahedron Lett. 51 (2010) 6403.